Pharmacological modulation of right ventricular endocardial-epicardial gradients in Brugada Syndrome

Justine Bhar-Amato MD*[1], Malcolm Finlay MD PhD* [2,5], Diogo Santos MSc[1], Michele Orini PhD[1], Sanjay Chaubey MD PhD[3], Vishal Vyas MD[2], Peter Taggart MD DSc[1], Andrew A. Grace MD PhD[4], Christopher L.-H. Huang MD PhD[4], Ron Ben-Simon MD[2], Andrew Tinker MD PhD[5], Pier D. Lambiase MD PhD[1,2]

Total Word Count 4841

*Joint first authorship

Affilliations:
1. **University College London (UCL)**
2. **Barts Heart Centre**
3. **Kings Collge London (KCL)**
4. **Cambridge University**
5. **Queens Mary's college London (QMUL)**

Addresses for Correspondence:

PD Lambiase
UCL Institute of Cardiovascular Science & Barts Heart Centre
Room 3.20
Rayne Institute,
5 University Street
London WC1E 6JF

43 **ABSTRACT**
44
45 **Background**

46 We explored the hypothesis that increased cholinergic tone exerts its pro-arrhythmic

47 effects in Brugada Syndrome (BrS) through increasing dispersion of transmural

48 repolarisation in patients with spontaneous and drug induced Brugada Syndrome.

49

50 **Methods**

51 BrS and Supraventricular tachycardia (SVT) patients were studied after deploying an

52 Ensite Array in the right ventricular outflow tract and a Cardima catheter in the great

53 cardiac vein to record endo & epicardial signals respectively. S_1-S_2 restitution curves from

54 the RV apex were conducted at baseline and after edrophonium challenge to promote

55 increased cholinergic tone. The local unipolar electrograms were then analyzed to study

56 transmural conduction and repolarisation dynamics.

57

58 **Results**

59 The study included 8 BrS patients: (5M: 3F; mean age 56y) and 8 controls patients with

60 SVT (5M: 3F; mean age 48y). Electrophysiological studies in controls demonstrated

61 shorter endocardial than epicardial right ventricular (RV) activation times (AT's) (mean

62 difference: 26 ms, p<0.001). In contrast, BrS patients showed longer endocardial than

63 epicardial AT (mean difference: -15 ms, p=0.001). BrS hearts, compared to controls,

64 showed significantly larger transmural gradients (TMG) in their activation recovery

65 intervals (ARIs) (mean intervals 20.5 vs 3.5 ms; p<0.01), with longer endocardial than

66 epicardial ARIs. Edrophonium challenge increased such gradients in both controls (to a

67 mean of 16 msecs (p<0.001) and BrS (to 29.7 ms; p<0.001). However, these were

68 attributable to *epicardial* and *endocardial* ARI prolongations in control and BrS hearts

69 respectively. Dynamic changes in repolarisation gradients were also observed across the

70 BrS RV wall in BrS.

71

72 **Conclusions:**

73 Differential contributions of conduction and repolarisation were identified in BrS which

74 critically modulated transmural dispersion of repolarisation with significant cholinergic

75 effects only identified in the BrS patients. This has important implications for explaining

76 the pro-arrhythmic effects of increased vagal tone in BrS aswell as evaluating autonomic

77 modulation & epicardial ablation as therapeutic strategies.

78

79 **Key Words:** Brugada Syndrome, Autonomic nervous system, Conduction, Repolarisation

80

81

82

83

84

85 **INTRODUCTION**
86
87 Brugada Syndrome (BrS) remains one of the most important causes of sudden cardiac

88 death in the young, accounting for 20% of such cases[1]. Its molecular basis remains

89 uncertain. Ion channel mutations primarily involving the sodium channel have only been

90 identified in up to 30% of subjects[2]. The pathophysiological basis for its associated

91 arrhythmias also remains contentious. BrS is characterised by a triad of right bundle

92 branch block (RBBB), coved ST elevation in the right precordial leads and lethal

93 ventricular arrhythmias. The disease appears localised to the right ventricle (RV) where

94 dynamic changes in ST elevation and ventricular arrhythmias develop in situations of

95 increased vagal tone.

96

97 High density intra-cardiac mapping by our group has identified significant conduction

98 delays in the RV outflow tract (RVOT) compared to the RV body and apex in BrS relative

99 to findings in control patients[3]. These data have been corroborated and it is now evident

100 that BrS is further associated with marked epicardial conduction abnormalities and

101 increased fibrosis[4-7]. Such fibrotic changes could lead to electrotonic uncoupling between

102 myocytes with source:sink mismatches between endocardium and epicardium. These

103   could produce the alterations in conduction or repolarisation gradients reported in a

104   recent mechanistic human study[8]. BrS has a more common nocturnal occurrence of

105   ventricular fibrillation which occurs in parallel with a corresponding nocturnal

106   accentuation of its pathognomonic ECG features[9]. These in turn correspond to the

107   increased vagal and diminished sympathetic activity during periods of rest[10]. However,

108   the electrophysiological effects of changes in autonomic tone on the BrS substrate remain

109   uncertain.

110   Here we explore the hypothesis that in BrS such increased cholinergic tone induces

111   conduction delay and promotes either intramural or transmural dispersions of

112   repolarisation in the RVOT. We evaluated the effect of cholinergic activation on in vivo

113   electrophysiological properties of the RV endocardium and RV epicardium in BrS patients.

114

115

METHODS

The data, analytic methods, and study materials will be made available to other researchers for purposes of reproducing the results or replicating the procedure on direct request.

Human electrophysiological mapping

The non-contact mapping study and pacing protocol were performed prior to ablation in the control patients or VT stimulation studies in the Brugada Syndrome (BrS) group. All anti-arrhythmic drugs had first been stopped for at least 5 half lives prior to the procedures. The detailed techniques for non-contact mapping in the ventricle are described elsewhere[11]. The multi-electrode array (MEA) (*Ensite,* St Jude Medical, St. Paul, Minnesota, USA) was deployed via the left femoral vein in the right ventricular outflow tract (RVOT) (full methodology described previously[3]). An epicardial 16-pole Pathfinder catheter (Cardima, California, USA) was passed into the distal great cardiac vein in the interventricular groove (Fig. 1). All patients gave informed consent and the study was approved by the University College London Hospital (UCLH) Research Ethics Committee.

Programmed ventricular stimulation was performed from the right ventricular apex. Three minutes of steady state pacing at a coupling interval of 400 ms was followed by a S_1S_2 restitution protocol using 400 ms drive trains. The extrastimulus was initially extended progressively by 50 ms intervals until consistent fusion with sinus beats occurred. The S_1S_2 interval was thereafter decreased at 20 ms intervals to 300 ms, then by 5 ms until the ventricular effective refractory period (VERP) was reached. The protocol was repeated following intravenous (IV) administration of 10 mg edrophonium to increase cholinergic tone, then followed by a 10 min washout period.

Offline analysis

140   24 virtual unipolar electrograms were placed in the RVOT in 4 columns of 6 virtuals to

141   obtain local endocardial data within 3 cm of the array directly opposite the position of the

142   16 pole Cardima catheter (Fig. 1). Endocardial & epicardial electrograms were exported

143   and analysed using semi-automated custom software running in Matlab (The Mathworks

144   Inc., MA, USA) (Figure S1). All electrograms and analyses were manually checked by 3

145   independent observers (JBA, MF, DS). The time from the earliest electrogram recorded

146   within the right ventricle (RV) to the steepest negative deflection (($dV/dt)_{min}$) was used as

147   the local activation time (AT). The sinus rhythm AT of the RV was taken as the time from

148   earliest to latest recorded RV activation. During pacing, the time from the pacing artefact

149   to the time corresponding to the ($dV/dt)_{min}$ was used as the local AT. Two methods have

150   been used to measure repolarisation times during non-contact mapping, respectively

151   termed the classical (Wyatt) method and the alternative method. Both have come under

152   intense theoretical and experimental scrutiny; here we present results using the classical

153   method[12-15]. Activation repolarisation interval (ARI), a well-validated approximation of

154   action potential duration, was defined as the interval between the AT and repolarization

155   time (Figure S1). The slope of ARI restitution was calculated using the least mean squares

156   method[16,17]. The RVOT was divided into 4 anatomical regions (anterior, posterior, lateral

157   septal), and activation and repolarisation dynamics were studied in the RVOT

158   endocardium and epicardium.

159   **Endocardial & Epicardial Regional Delay**

160   Mean increase of delay (MID) was calculated by dividing the integrated increase of delay

161   (area under the curve) by the interval between baseline cycle length and the refractory

162   period.[18] The degree of delay was measured from 4 segments in the RVOT and in the

163   epicardium.

Genetic testing

Blood samples (10 mL) were obtained from participating BS subjects. Genomic DNA was isolated from peripheral blood leukocytes with the use of a commercial kit (Gentra System, Puregene). The exons of SCN5A were amplified and analyzed by direct sequencing. Polymerase chain reaction products were purified with Exosap (USB) and were directly sequenced from both directions with the ABI PRISM BigDye Terminator Cycle Sequencing Reaction and the ABI PRISM 3130XL Automatic DNA Sequencer.

Statistical analysis

Statistical computing was performed using R software (The Comprehensive R Archive Network (CRAN)). Comparisons in which a single measurement was taken for each subject, e.g. steady state AT, ARI, RT, Smax, MID, maximum endo-epicardial differences were compared with a Kruskal Wallis non-parametric test with post-hoc correction for multiple comparisons (Dunn).

Electrogram data were modelled with the use of mixed effects linear regression (software, MLwIN version 2.01), and statistical significance was inferred from the model. The AT, ARI, RT restitution curve data were compared with the use of curve fitting. MLwIN was used to fit a regression model to the restitution curve data, and statistical significance was inferred from the model fit. Quartile regression with bootstrapping (Quantile Regression Description Estimation and inference (QUANTREG) package) was used to compare non-parametric continuous data.

RESULTS

Mapping was performed in 16 patients (BrS group: n = 8, 5M: 3F; mean age 56 y, control group: n=8, 5M: 3F; mean age 48,). The demographic data is shown in Table 1. Four BrS patients had resting type 1 ECGs and two had a family history of sudden cardiac death. No

189   significant structural abnormalities were detected on echocardiography or MRI with MRI

190   excluding gadolinium late enhancement or T1 mapping abnormalities in the right and left

191   ventricles in the 4 scanned cased. Only one patient had an ICD inserted for symptomatic

192   non-sustained VT and none have had any significant ventricular arrhythmic events in 8

193   years of follow-up.

194

195   Genetic data are available in 4 subjects: BrS cases 3-5 were negative for known pathogenic

196   SCN5A mutations and BrS subject 8 was a carrier of a c.3045_3046delGA, exon 17 SCN5A,

197   which is predicted to cause a frameshift of the amino acid sequence in leading to a

198   premature termination of translation.

199

200   The control group of patients had SVT (Table 1). They had normal resting and signal

201   averaged ECGs, a negative ajmaline challenge test, structurally normal hearts on

202   echocardiography and no family history of sudden cardiac death. Informed consent was

203   obtained following local research ethics committee approval. We used the

204   acetylcholinesterase inhibitor edrophonium to activate muscarinic receptors.

205

206   We made direct measurements of epicardial and endocardial activation times (AT), and

207   activation recovery intervals (ARI), from which we further derived recovery times (RTs)

208   in both control and BrS patients before and following autonomic edrophonium challenge.

209   This permitted us to derive the transmural gradients in AT, ARI and RTs, relating these

210   phenotypic characteristics to findings in BrS or normal patients.

211   During **steady pacing**, epicardial **activation times (**ATs) and **activation recovery**

212   **intervals (**ARIs) and **repolarisation times (**RTs) were significantly shorter in BrS than in

213   control patients. Neither epicardial AT and ARIs were significantly affected by

214   edrophonium challenge (Table 2, Fig. S2). In contrast, endocardial RTs were significantly

215   longer in BrS than control patients, and similarly only minimally affected by edrophonium

216   challenge.

217   Measurements made through **_varying coupling intervals used to construct restitution_**

218   **_curves_** demonstrated that control patients showed shorter endocardial than epicardial

219   ATs that gave mean AT differences of 26 ms, 95% CI: 21, 32 for endocardium and

220   epicardium respectively, $p<0.001$(Table 2, Fig. 2). In contrast, the BrS patients showed

221   longer endocardial AT than epicardial AT (mean AT difference: 15 ms, 95% CI 11, 20, for

222   endocardium and epicardium respectively; $p=0.001$). Following edrophonium challenge,

223   both endocardial and epicardial ATs were unchanged in the control but significantly

224   further shortened in the BrS patients. However, neither control nor BrS patients showed

225   significant changes in their transmural activation time differences. When we measured the

226   regional delay to assess conduction reserve, this was greater in the epicardium than endocardium

227   in BrS versus controls and was further exaggerated following edrophonium (Table 2, Fig. 3).

228

229   Hearts from the control patients showed minimal transmural gradients (TMG) in their

230   ARIs (mean 3.4 ms, 95% CI: 0.0, 6.8, $p<0.05$) with endocardial ARIs that were marginally

231   shorter than epicardial ARIs (Table 2, Fig. 4). In contrast, hearts from the BrS patients

232   showed significantly larger TMG (mean 20.5 ms, 95% CI: 15.5, 25.5, $p<0.001$), with shorter

233   epicardial ARIs than endocardial ARIs.

234   Following edrophonium challenge, the TMG in hearts from control patients increased to a

235   mean of 16 ms (95% CI: 12.6, 19.6, $p<0.001$), and this reflected an _epicardial_ ARI

236   prolongation. The TMG in hearts from BrS patients increased to 29.7 ms (95% CI: 24.1,

237   35.3, $p<0.001$), but this reflected _endocardial_ as opposed to epicardial ARI prolongation.

238   These effects were particularly evident from contact endocardial and epicardial

239   electrogram recordings illustrating the unipolar electrogram morphologies in hearts from

240   BrS versus control patients and the effects of edrophonium on the degree of ST elevation

241   in the epicardium (Fig. 5).

242
243   In control patients, epicardial repolarisation as reflected in its ***repolarisation times (RT)***

244   was completed later than endocardial repolarisation (Table 2, Fig 6). The resulting RT

245   gradient therefore ran from epi- to endocardium. However, in the BrS patients, epicardial

246   repolarisation was completed earlier than endocardial repolarisation and showed smaller

247   values at long cycle lengths. This resulted in a reversed RT gradient with significantly

248   shorter epicardial versus endocardial RTs. Edrophonium challenge left the RT gradient

249   flat and unaffected across all the coupling intervals in the control patients. In contrast, in

250   the BrS patients, edrophonium challenge resulted in a significant increase in the epicardial

251   RTs which was most pronounced at longer CI's. The RT gradients across the coupling

252   intervals altered particularly at shorter intervals (Fig. 6).

253

254   ***Maximum ARI restitution slopes***

255   Endocardial & epicardial maximum ARI restitution slopes (S_{max}) at baseline were

256   equivalent however post edrophonium endocardial Smax were increased in hearts of BrS

257   patients (0.75 vs 0.5 P<0.0001)) compared with control patients (Table 2, Figure 7).

258   Edrophonium significantly increased the endocardial–epicardial S_{max} differences in hearts

259   from control patients and marginally steepened endocardial BrS Smax. No significant

260   changes in Smax occurred epicardially in both groups.

261

262   **Discussion**

263   We report the first detailed *in vivo* investigation of the effects of autonomic modulation on

264   right ventricular endocardial and epicardial electrophysiology in BrS. This revealed that

265   the modulation of activation and repolarisation gradients by premature stimuli may be

266   greater in BrS.

267

268   Our studies determined epicardial and endocardial activation times (AT), activation

269   recovery intervals (ARI), and recovery times (RTs) in both control and BrS patients. From

270   these we derived the corresponding transmural gradients in AT, ARI and RTs before and

271   following autonomic edrophonium challenge and related these phenotypic characteristics

272   to findings in BrS or normal patients. We observed significant effects of both *absolute and*

273   *transmural differences* between both conduction and repolarisation characteristics and

274   differing effects upon these of cholinergic challenge. We thus associated differences in the

275   spatial organisation and heterogeneity of these changes in activation and repolarisation

276   with the BrS condition.

277   Our key findings concerned abnormalities in the transmural gradients of both activation

278   and repolarisation in Brugada syndrome patients and their accentuation by cholinergic

279   stimulation. Thus, whereas in control individuals, the epicardium completed

280   repolarisation before the endocardium, in BrS this sequence was reversed. Edrophonium

281   modulated the abnormal transmural gradient in BrS leading to further delayed epicardial

282   repolarisation.   This reflected differential effects of the BrS condition and of cholinergic

283   challenge upon conduction velocity and repolarisation which govern the transmural

284   activation sequence. Thus, prior to cholinergic challenge, the main differences between

285   human BrS and controls reflected epicardial differences with the BrS showing shorter

286   ARI's and the epicardium activating earlier than the endocardium. This parallels the

287   findings of other groups[7,8, 19]. Indeed the largest mean ARI gradient at rest is equivalent:

288   20.5ms versus 24ms in the Langendorrff study of a Brugada heart[19]. This causes a

289   significant reversed repolarisation gradient to arise from endocardium to epicardium

290   which did not exist in controls. Increased cholinergic tone through edrophonium

291   administration exerted additional important effects on conduction-repolarisation

292   dynamics in BrS with significant differences in epi and endocardial electrophysiological

293   responses. There is a reversed ARI gradient in BrS patients with shorter epicardial ARI's

294   compared with a smaller opposite ARI gradient in normal individuals at baseline. These

295   differences are exacerbated by increased cholinergic tone with preferential endocardial

296   ARI prolongation in BrS. Furthermore, edrophonium steepened Smax in the endocardium

297   in BrS which would promote the risk of VF as steepening of ARI restitution slopes

298   promotes the probability of wavebreak and re-entry[3].

299

300   The findings may reflect a differential distribution of ion channels between the

301   endocardium and epicardium[20]. Differences in sodium channel, calcium channel and

302   potassium channel expression and differential regulation of currents by autonomic

303   pathways are likely to account for the striking endo and epicardial differences. This

304   indicates a loss of endocardial to epicardial conduction reserve which could be due to

305   abnormalities in the Purkinje network preventing rapid endocardial tissue recruitment

306   and subsequent endo–epicardial depolarisation as well as reduced tissue coupling

307   secondary to lack of Na channel recruitment (excitability) and tissue fibrosis.

308

309   The data also show that increased cholinergic tone promotes heterogeneity between epi

310   and endocardium and suggests the main cholinergic effects in BrS are exerted on the

311   endocardial ARI, combined with conduction delays *amplifying transmural repolarisation*

312   *dynamic differences across coupling intervals.* The marked conduction delays especially at

313   short coupling intervals in these studies in conjunction with the shorter ARI's in the

314   Brugada heart create the optimal conditions to promote large endo-epicardial conduction

315   and repolarisation gradients.

316

317   The electrophysiological changes reported here may also bear upon the "conduction and

318   repolarisation hypotheses" explaining the characteristic clinical ECG waveform in BrS[21].

319   These variously explain its coved ST elevation by delayed depolarisation from the RV body

320   to RVOT or transmural gradients in repolarisation secondary to a shortened "dip and

321   plateau" action potential morphology in the epicardium. The present findings are

322   consistent with a combination of these mechanisms. This would be compatible with the

323   differential conduction delay between the endocardium and epicardium and the earlier

324   epicardial repolarisation in BrS. Furthermore, changes in coupling interval modulate these

325   features on a beat to beat basis, and this would promote the creation of endocardial-

326   epicardial repolarisation gradients and hence ST elevation in the right precordial leads

327   with the gradients particularly in the presence of electrotonic uncoupling promoted by

328   structural abnormalities[22,23].

329

330   The findings also have implications for electrocardiographic changes following conditions

331   of increased cholinergic tone in BrS. Thus, increased vagal tone is known to produce

332   dynamic changes in J point elevation and ventricular arrhythmia. Nakazawa et al. reported

333   that high vagal tone and low sympathetic tone are specific properties of symptomatic BrS

334   on the basis of heart rate variability data [24]. Their study also suggested these autonomic

335   imbalances were significant in the symptomatic group but not in the asymptomatic group.

336   Dynamic changes in J point elevation are more prominent at night particularly in patients

337   with previous VF. Abnormal 123I-MIBG uptake in patients with BrS is described indicating

338   presynaptic sympathetic dysfunction of the heart shifting the influence to increases in

339   cholinergic tone[25]. The precise relationship between vagal tone and pro-arrhythmia is

340   subject to debate. Increased vagal tone is thought to reduce the Ca transient during phase

341   2 of the action potential resulting in increased transmural dispersion of repolarisation and

342   phase 2 re-entry[26]. The data supporting this hypothesis has been derived from the canine

343   RV wedge preparation of BrS employing pharmacological manipulations to reproduce the

344   Brugada ECG.

345   This study demonstrates that autonomic effects are 2-fold-promoting endocardial ARI

346   prolongation with marked shortening of endo and epicardial AT. These 2 effects will be

347   highly pro-arrhythmic enabling endocardial functional conduction block and promoting a

348   large vulnerable window epicardially to facilitate re-entry.

349   **Limitations**

350   We were unable to biopsy the sites of recording or undertake direct epicardial recording

351   of the substrate so it is possible that more severely diseased areas were not studied.

352   Nevertheless, these findings indicate sufficient pathology was present to enable significant

353   differences in conduction-repolarisation dynamics to be identified. These findings provide

354   evidence of conduction-repolarisation abnormalities in BrS without events but the extent

355   of such changes need to be explored in more severely affected individuals as there is

356   preliminary evidence to suggest that such cases may have more marked conduction

357   abnormalities using ECG Imaging[27,28]. Indeed the extent of these changes could be used as

358   a risk marker for lethal arrhythmias.

359

360   These data have important clinical implications with recent interest in epicardial

361   substrate ablation to prevent VF in BrS[29,30]. Ablation appears to normalise the resting ECG

362   and prevent dynamic ST elevation. This may operate by homogenising the substrate such

363   that endo and epicardial gradients can no longer be generated in the RVOT. This will

364   prevent changes in cholinergic tone influencing the gradient & enabling VF initiation if

365   these transmural gradients are primarily responsible for arrhythmogenesis.

366

375

376   **Disclosure Statement:**

377   None

378

References

1. Silvia G. Priori, Arthur A. Wilde, Minoru Horie, Yongkeun Cho, Elijah R. Behr, Charles Berul, Nico Blom, Josep Brugada, Chern-En Chiang, Heikki Huikuri, Prince Kannankeril, Andrew Krahn, Antoine Leenhardt, Arthur Moss, Peter J. Schwartz, Wataru Shimizu, Gordon Tomaselli, Cynthia Tracy, Executive Summary: HRS/EHRA/APHRS Expert Consensus Statement on the Diagnosis and Management of Patients with Inherited Primary Arrhythmia Syndromes, *Heart Rhythm*. 2013; 10:e85-e108.

2. Bezzina CR, Lahrouchi N, Priori SG, Genetics of sudden cardiac death, *Circ Res.* 2015; 116:1919-36.

3. Lambiase PD, Ahmed AK, Ciaccio EJ, Brugada R, Lizotte E, Chaubey S, Ben-Simon R, Chow AW, Lowe MD, McKenna WJ. High-density substrate mapping in Brugada syndrome: combined role of conduction and repolarization heterogeneities in arrhythmogenesis. *Circulation*. 2009; 120:106–17.

4. Postema PG, van Dessel PF, de Bakker JM, Dekker LR, Linnenbank AC, Hoogendijk MG, Coronel R, Tijssen JG, Wilde AA, Tan HL. Slow and discontinuous conduction conspire in Brugada syndrome: a right ventricular mapping and stimulation study. *Circ Arrhythm Electrophysiol*. 2008; 1:379–86.

5. Nademanee K, Raju H, de Noronha SV, Papadakis M, Robinson L, Rothery S, Makita N, Kowase S, Boonmee N, Vitayakritsirikul V, Ratanarapee S, Sharma S, van der Wal AC, Christiansen M, Tan HL, Wilde AA, Nogami A, Sheppard MN, Veerakul G, Behr ER. Fibrosis, Connexin-43, and Conduction Abnormalities in the Brugada Syndrome. *J Am Coll Cardiol*, 2015; 66:1976-86.

6. Ohkubo K, Watanabe I, Okumura Y, Takagi Y, Ashino S, Kofune M, Sugimura H, Nakai T, Kasamaki Y, Hirayama A, Morimoto S.. Right ventricular histological substrate and conduction delay in patients with Brugada syndrome. *Int Heart J.* 2010; 51:17–23.

7. Frustaci A, Priori SG, Pieroni M, Chimenti C, Napolitano C, Rivolta I, Sanna T, Bellocci F, Russo MA.. Cardiac histological substrate in patients with clinical phenotype of Brugada syndrome. *Circulation.* 2005; 112:3680–7.

8. Ten Sande JN, Coronel R, Conrath CE, Driessen AH, de Groot JR, Tan HL, Nademanee K, Wilde AA, de Bakker JM, van Dessel PF ST-Segment Elevation and Fractionated Electrograms in Brugada Syndrome Patients Arise From the Same Structurally Abnormal Subepicardial RVOT Area but Have a Different Mechanism. *Circ Arrhythm Electrophysiol.* 2015; 1382-92.

9. Matsuo K, Kurita T, Inagaki M, Kakishita M, Aihara N, Shimizu W, Taguchi A, Suyama K, Kamakura S, Shimomura K. The circadian pattern of the development of ventricular fibrillation in patients with Brugada syndrome. *Eur Heart J.* 1999; 20:465-70.

10. Mizumaki K, Fujiki A, Tsuneda T, Sakabe M, Nishida K, Sugao M, Inoue H. Vagal activity modulates spontaneous augmentation of ST elevation in the daily life of patients with Brugada syndrome. *J Cardiovasc Electrophysiol.* 2004; 15:667-73.

11. Schilling RJ, Davies DW, Peters NS. Characteristics of sinus rhythm electrograms at sites of ablation of ventricular tachycardia relative to all other sites: a noncontact mapping study of the entire left ventricle. *J Cardiovasc Electrophysiol.* 1998; 9:921–933.

12. Franz MR, Bargheer K, Rafflenbeul W, Haverich A, Lichtlen PR. Monophasic action potential mapping in human subjects with normal electrocardiograms: direct evidence for the genesis of the T wave. *Circulation.* 1987; 75:379-86.

13. Yue AM, Paisey JR, Robinson S, Betts TR, Roberts PR, Morgan JM. Determination of human ventricular repolarization by noncontact mapping: validation with monophasic action potential recordings. *Circulation*. 2004; 110:1343-50.

14. Potse M, Coronel R, Opthof T, Vinet A. The positive T wave. *Anadolu Kardiyol Derg*. 2007; 1:164-7.

15. Potse M, Vinet A, Opthof T, Coronel R. Validation of a simple model for the morphology of the T wave in unipolar electrograms. *Am J Physiol Heart Circ Physiol.* 2009; 297:792-801.

16. Taggart P, Sutton P, Chalabi Z, Boyett MR, Simon R, Elliott D, Gill JS. Effect of adrenergic stimulation on action potential duration restitution in humans. *Circulation*. 2003; 107:285-9.

17. Hanson B, Sutton P, Elameri N, Gray M, Critchley H, Gill JS, Taggart P. Interaction of activation-repolarization coupling and restitution properties in humans. *Circ Arrhythm Electrophysiol*. 2009; 2:162-70.

18. Kawara T, Derksen R, de Groot JR, Coronel R, Tasseron S, Linnenbank AC, Hauer RN, Kirkels H, Janse MJ, de Bakker JM. Activation delay after premature stimulation in chronically diseased human myocardium relates to the architecture of interstitial fibrosis. *Circulation*. 2001; 104:3069–3075

19. Coronel R, Casini S, Koopmann TT, Wilms-Schopman FJ, Verkerk AO, de Groot JR, Bhuiyan Z, Bezzina CR, Veldkamp MW, Linnenbank AC, van der Wal AC, Tan HL, Brugada P, Wilde AA, de Bakker JM. Right ventricular fibrosis and conduction delay in a patient with clinical signs of Brugada syndrome: a combined electrophysiological, genetic, histopathologic, and computational study. *Circulation*. 2005; 112:2769–2777.

20. 21. Opthof T, Remme CA, Jorge E, Noriega F, Wiegerinck RF, Tasiam A, Beekman L, Alvarez-Garcia J, Munoz-Guijosa C, Coronel R, Cinca J.. Cardiac activation-

repolarization patterns and ion channel expression mapping in intact isolated normal human hearts. *Heart Rhythm*. 2017; 14:265-272.

21. Meregalli PG, Wilde AA, Tan HL. Pathophysiological mechanisms of Brugada syndrome: depolarization disorder, repolarization disorder, or more? *Cardiovasc Res*. 2005; 67:367-78.

22. Hoogendijk MG, Potse M, Linnenbank AC, Verkerk AO, den Ruijter HM, van Amersfoorth SC, Klaver EC, Beekman L, Bezzina CR, Postema PG, Tan HL, Reimer AG, van der Wal AC, Ten Harkel AD, Dalinghaus M, Vinet A, Wilde AA, de Bakker JM, Coronel R. Mechanism of right precor- dial ST-segment elevation in structural heart disease: excitation failure by current-to-load mismatch. *Heart Rhythm*. 2010; 7:238–248.

23. Hoogendijk MG, Potse M, Vinet A, de Bakker JM, Coronel R. ST segment elevation by current-to-load mismatch: an experimental and computational study. *Heart Rhythm*. 2011; 8:111–118.

24. Nakazawa K, Sakurai T, Takagi A, Kishi R, Osada K, Nanke T, Miyake F, Matsumoto N, Kobayashi S. Autonomic imbalance as a property of symptomatic Brugada syndrome. *Circ J*. 2003; 67:511-4.

25. Wichter T, Matheja P, Eckardt L, Kies P, Schäfers K, Schulze-Bahr E, Haverkamp W, Borggrefe M, Schober O, Breithardt G, Schäfers M. Cardiac autonomic dysfunction in Brugada syndrome. *Circulation*. 2002; 105:702-6.

26. Yan GX, Antzelevitch C. Cellular basis for the Brugada syndrome and other mechanisms of arrhythmogenesis associated with ST-segment elevation. *Circulation.* 1999; 100:1660–6.

27. Leong KMW, Ng FS, Yao C, Roney C, Taraborrelli P, Linton NWF, Whinnett ZI, Lefroy DC, Davies DW, Boon Lim P, Harding SE , Peters NS, Kanagaratnam P, Varnava AM. ST-

Elevation Magnitude Correlates With Right Ventricular Outflow Tract Conduction Delay in Type I Brugada ECG. *Circ Arrhythm Electrophysiol.* 2017;10:e005107.

28. Leong KMW Ng FS, Roney C, Cantwell C, Shun-Shin MJ, Linton NWF , Whinnett ZI, Lefroy DC, Davies DW, Harding SE, Lim PB, Francis D, Peters NS, Varnava AM, Kanagaratnam P. Repolarization abnormalities unmasked with exercise in sudden cardiac death survivors with structurally normal hearts. *J Cardiovasc Electrophysiol.* 2018; 29:115-126.

29. Nademanee K, Veerakul G, Chandanamattha P, Chaothawee L, Ariyachaipanich A, Jirasirirojanakorn K, Likittanasombat K, Bhuripanyo K, Ngarmukos T. Prevention of ventricular fibrillation episodes in Brugada syndrome by catheter ablation over the anterior right ventricular outflow tract epicardium. *Circulation.* 2011; 123:1270-9.

30. Pappone C, Brugada J, Vicedomini G, Ciconte G, Manguso F, Saviano M, Vitale R, Cuko A, Giannelli L, Calovic Z, Conti M, Pozzi P, Natalizia A, Crisà S, Borrelli V, Brugada R, Sarquella-Brugada G, Guazzi M, Frigiola A, Menicanti L, Santinelli V.Electrical Substrate Elimination in 135 Consecutive Patients With Brugada Syndrome. *Circ Arrhythm Electrophysiol.* 2017;10:e005053.

Table 1. Study Patient Characteristics

Study No BrS/Control	Age	Sex	FHx SCD	Spont.Type 1 ECG	Previous VT/VF	VT Stim	Late Potentials	ICD	Imaging	Genetics
BrS1	51	M	-	-	-	+	-	-	Normal Echo	
BrS2	49	M	-	+	-	-	+	-	Normal Echo	
BrS3	59	M	+	-	-	-	-	-	Normal Echo	
BrS4	62	M	-	+	-	-	+	-	Normal Echo	
BrS5	45	F	-	-	+	-	-	+	Normal MRI-No Gd & Normal T1	
BrS6	51	M	-	+	-	-	+	-	Normal MRI-No Gd & Normal T1	
BrS7	55	M	-	+	-	-	-	-	Mild concentric LVH-No Gd & Normal T1	
BrS8	79	F	+	-	-	-	+	-	Normal MRI-No Gd & Normal T1	SCN5A+ -Exon 17
			Diagnosis							
C1	74	M	Arial Flutter							
C2	55	F	AVNRT							
C3	40	F	AVRT							
C4	49	M	AVRT							
C5	49	M	AVNRT							
C6	39	M	AVNRT							
C7	28	F	AVNRT							

Table 2. Endo and Epicardial Conduction and Repolarisation Parameters

AT(ms) – Activation Time; ARI(ms) – Activation-Recovery-Interval; RT(ms) – Repolarization Time; Smax – Maximum Slope ARI Restitution Curve; MID(ms) – Mean Increase Delay
*P<0.05 Ep-Epi differences Control Edr vs BrS Edr. *** P<0.001 Control vs BrS Endo after Edr.
† Kruskal Wallis test with Dunn's multiple comparisons test. ‡ mixed effects linear regression

Parameter	Control (n=8)	BrS (n=8)		Control+EDR (n=8)	BrS+EDR (n=8)	
Baseline	Median (lower quartile, upper quartile)	Median (lower quartile, upper quartile)	P †	Median (lower quartile, upper quartile)	Median (lower quartile, upper quartile)	P †
Endocardial						
AT	70.8 (58.8, 85.3)	77.8 (69.4, 90.1)	ns	60.8 (53.1, 80.0)	74.5 (59.3, 81.6)	ns
ARI	209.6 (182.0, 231.9)	214.8 (166.9, 227.5)	ns	209.1 (198.8, 219.2)	215.2 (180.9, 230.9)	ns
RT	251.8 (226.3, 269.6)	293.2 (260.3, 312.8)	0.005	248.9 (225.3, 272.0)	287.8 (272.5, 302.1)	0.0003
Epicardial						
AT	109.8 (78.3, 121.1)	65.5 (43.3, 98.6)	< 0.0001	92.3 (64.0, 124.8)	62.3 (51.7, 90.9)	< 0.0001
ARI	210.0 (197.5, 216.5)	183.8 (168.2, 191.6)	< 0.0001	218.1 (198.2, 236.1)	181.5 (165.3, 194.1)	< 0.0001
RT	322.0 (272.0, 335.6)	275.3 (237.7, 296.9)	< 0.0001	309.2 (257.1, 339.1)	276.3 (230.7, 306.4)	0.003
Restitution Curves	Median (lower quartile, upper quartile)	Median (lower quartile, upper quartile)	P (of Entire curve) ‡	Median (lower quartile, upper quartile)	Median (lower quartile, upper quartile)	P (of Entire curve) ‡
Endocardial (over 600-1000ms coupling Interval)						
AT	79.2 (75.2, 87.6)	83.6 (82.2, 96.7)	ns	72.8 (66.2, 81.4)	74.8 (67.6, 81.2)	ns
ARI	208.9 (201.3, 227.5)	233.8 (211.1, 247.9)	ns	221.3 (204.0, 227.1)	247.1 (212.5, 252.9)	ns
RT	269.7 (265.6, 276.4)	333.7 (323.4, 341.0)	< 0.0001	267.3 (264.2, 270.1)	316.3 (300.0, 323.3)	< 0.0001
Epicardial (over 600-1000ms coupling Interval)						
AT	116.3 (87.9, 118.7)	56.6 (55.9, 64.2)	< 0.0001	121.0 (105.0, 123.4)	53.6 (48.9, 59.4)	< 0.0001
ARI	225.8 (207.8, 232.5)	217.8 (209.1, 226.6)	< 0.0001	243.8 (223.8, 262.4)	222.2 (208.8, 233.3)	< 0.0001
RT	334.5 (328.3, 343.3)	289.9 (277.8, 293.5)	< 0.0001	346.3 (335.5, 352.1)	307.5 (282.4, 310.0)	< 0.0001
Endocardial			P †			P †
Smax	0.6 (0.5, 0.9)	0.7 (0.6, 0.8)	ns	0.5 (0.4, 0.7)	0.7 (0.6, 09)	< 0.0001
MID	1.7 (0.5, 2.8)	1.2 (0.7, 1.6)	ns	1.7 (0.9, 2.7)	1.6 (1.1, 2.0)	ns
Epicardial						
Smax	0.7 (0.4, 0.8)	0.8 (0.5, 1.2)	ns	0.7 (0.5, 0.9)	0.7 (0.5, 1.2)	ns
MID	2.1 (1.6, 2.8)	2.0 (1.3, 3.3)	ns	2.1 (1.6, 3.3)	3.1 (2.3, 3.7)	<0.05
Endo-Epicardial Differences	Mean (95% CI)	Mean (95% CI)		Mean (95% CI)	Mean (95% CI)	
AT	-26 (-21, -32)	15 (11, 20)		-36.2 (-26.4, -46.1)	2.5 (12.2, -7.1)*	
P ‡	P<0.001	P=0.001		< 0.0001	Ns	
ARI	-3.4 (0.0, -6.8)	20.5 (15.5, 25.5)		-16 (-12.6, -19.6)	29.7 (24.1, 35.3)	
P ‡	P<0.05	P<0.001		P<0.001	P<0.001	
RT	-36.4 (-25.9, -46.8)	30.6 (41.9, 19.4)		-50.8 (-39.8, -61.7)	32.4 (44.1, 20.6)	
P ‡	< 0.0001	< 0.0001		< 0.0001	< 0.0001	
Smax (P †)	ns	0.001		0.002***	ns	
MID (P †)	ns	0.001		<0.05	0.0002	

Figure Legends

Figure 1. Positioning of Mapping Catheters in the RV and great cardiac vein to record RV endocardial and epicardial electrograms.

Figure 2. Endo and Epicardial Activation time dynamics pre and post edrophonium in control and Brugada hearts.

Figure 3

Boxplots representing the mean increase delay (MID), endocardially (Endo) and epicardially (Epi), for both Control and Brugada subjects, before (Base) and after Edrophonium (Edr) administration. For the control group, a significant difference in the MID between endocardial and epicardial regions was induced by drug administration. For the Brugada group, a significant difference was already present at baseline and was further exacerbated. These differences were mainly due to a MID prolongation in the epicardium. *P<0.05 **P<0.01 ***P<0.001

Figure 4. Endo and Epicardial ARI dynamics pre and post edrophonium in control and Brugada Hearts.

Figure 5. Example of Sinus rhythm ECG and Electrograms Recorded epi and endocardially in a Control and BrS patient. There is a type II coved ST elevation pattern resting ECG of the BrS patient which Is reflected in the epicardial unipolar electrograms-these are exaggerated after edrophonium (blue) as well as a decrease in activation times in the epicardial electrograms. No significant change occurs in the control after the edrophonium.

Figure 6. Endo and Epicardial Repolarisation Time dynamics pre and post edrophonium in control and Brugada Hearts. P values represent the differences between the curves pre and post edroponium in each group.

Figure 7.

Boxplots representing the maximum ARI restitution slopes under each condition (Smax), endocardially (Endo) and epicardially (Epi), for both Control and Brugada subjects, before (Base) and after Edrophonium (Edr) administration. For the control group, a significant difference in the Smax between endocardial and epicardial regions was induced by drug administration. For the Brugada group, a significant difference was present at baseline. *P<0.05 **P<0.01 ***P<0.001
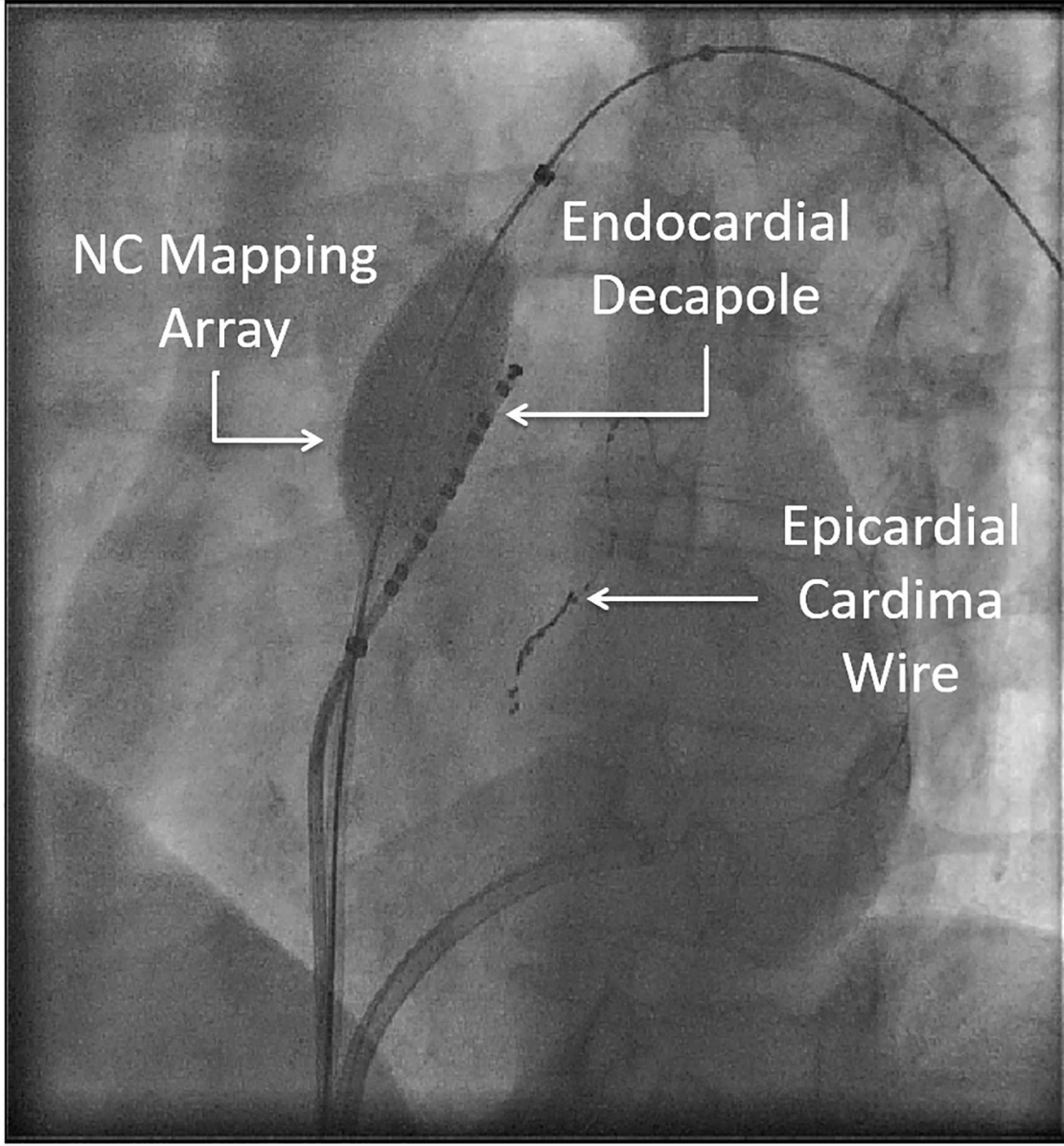
Control | BrS

ECG - V1
ECG - V2
ECG - V3
Epi - CS2
Epi - CS4
Endo - Virt 2
Endo - Virt 4
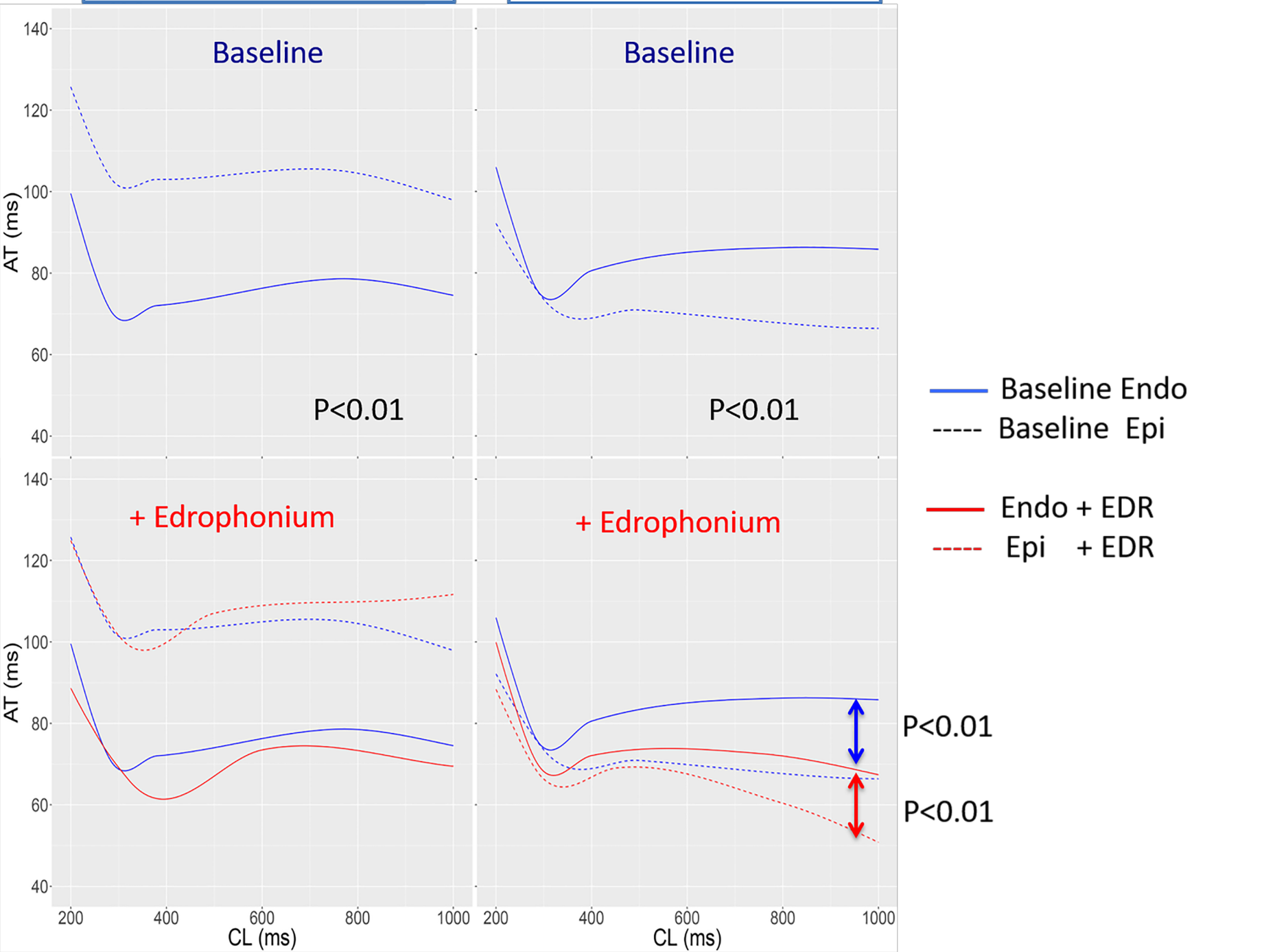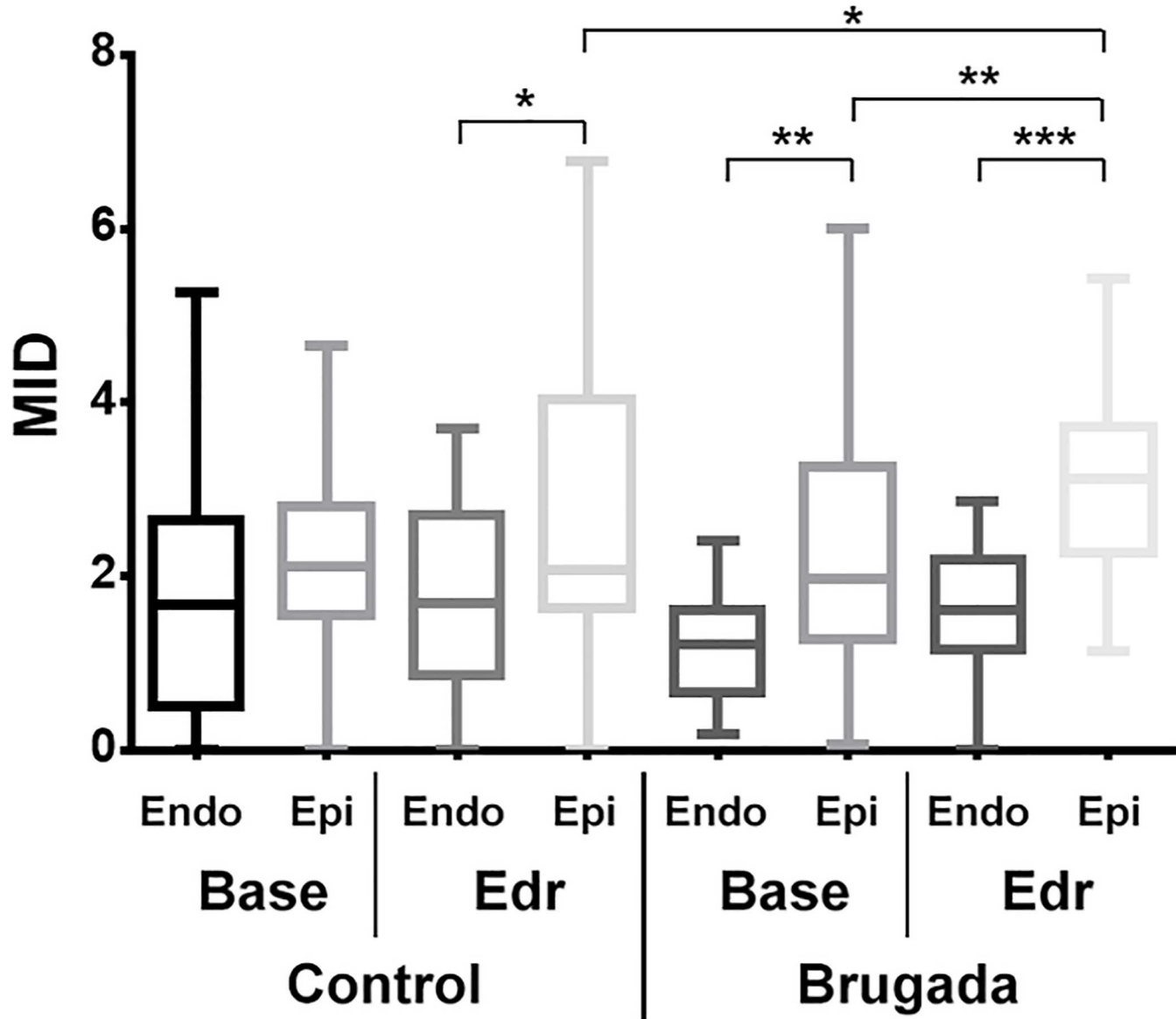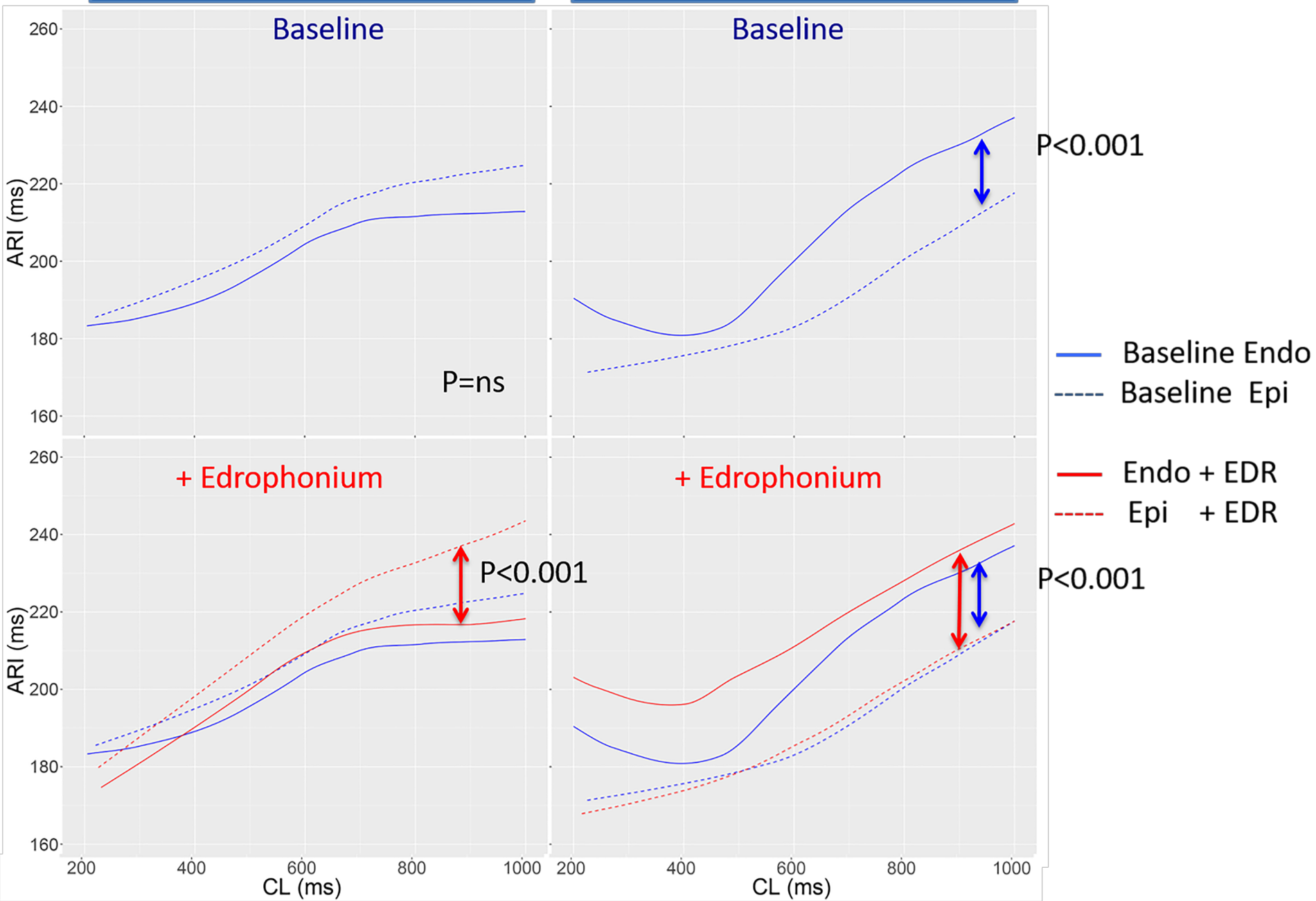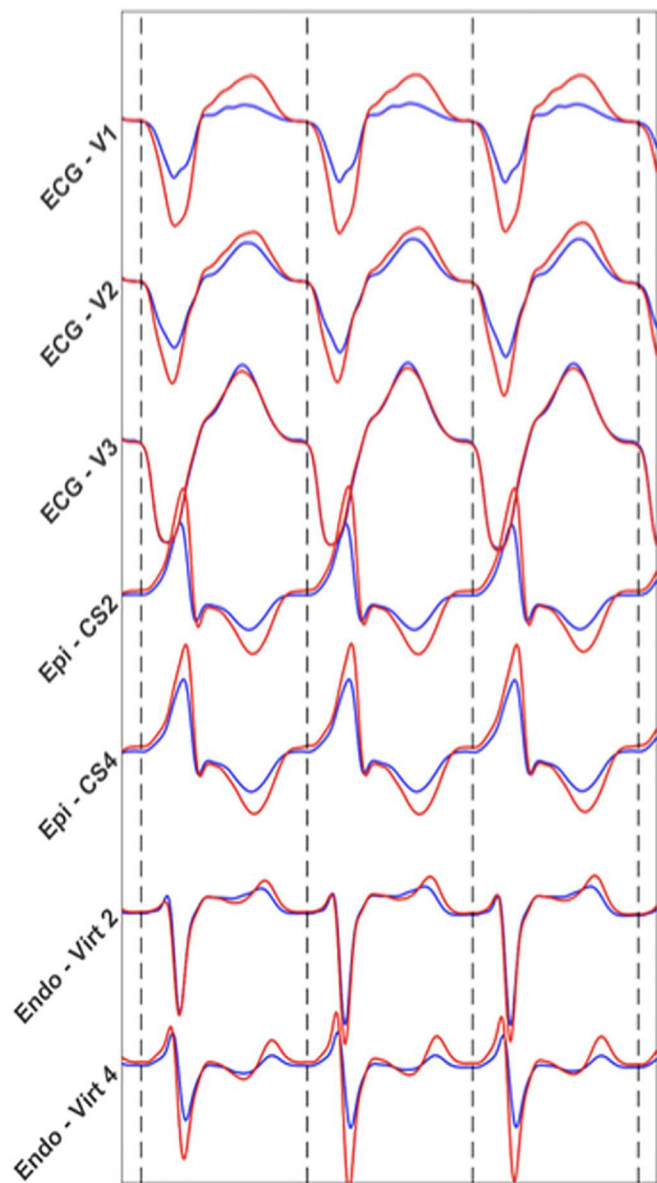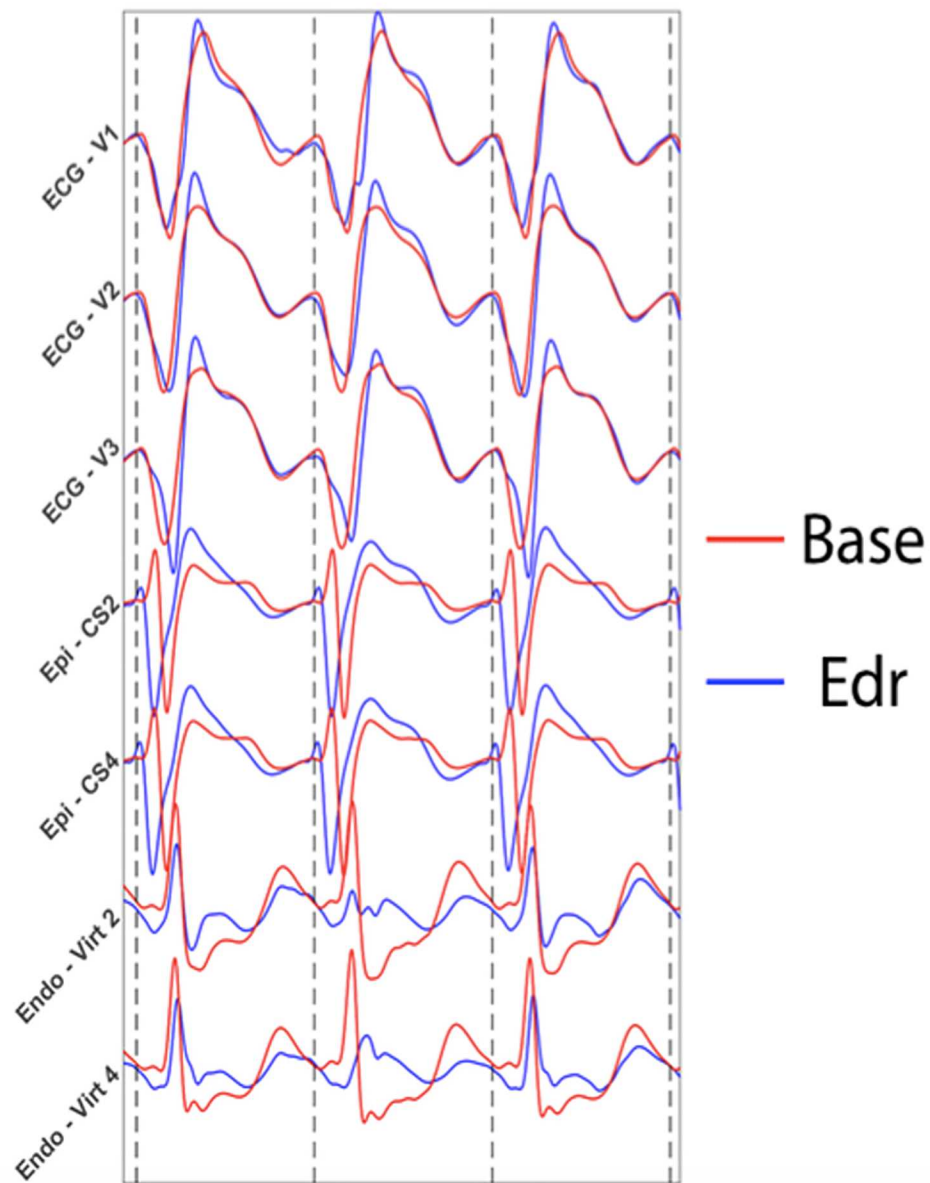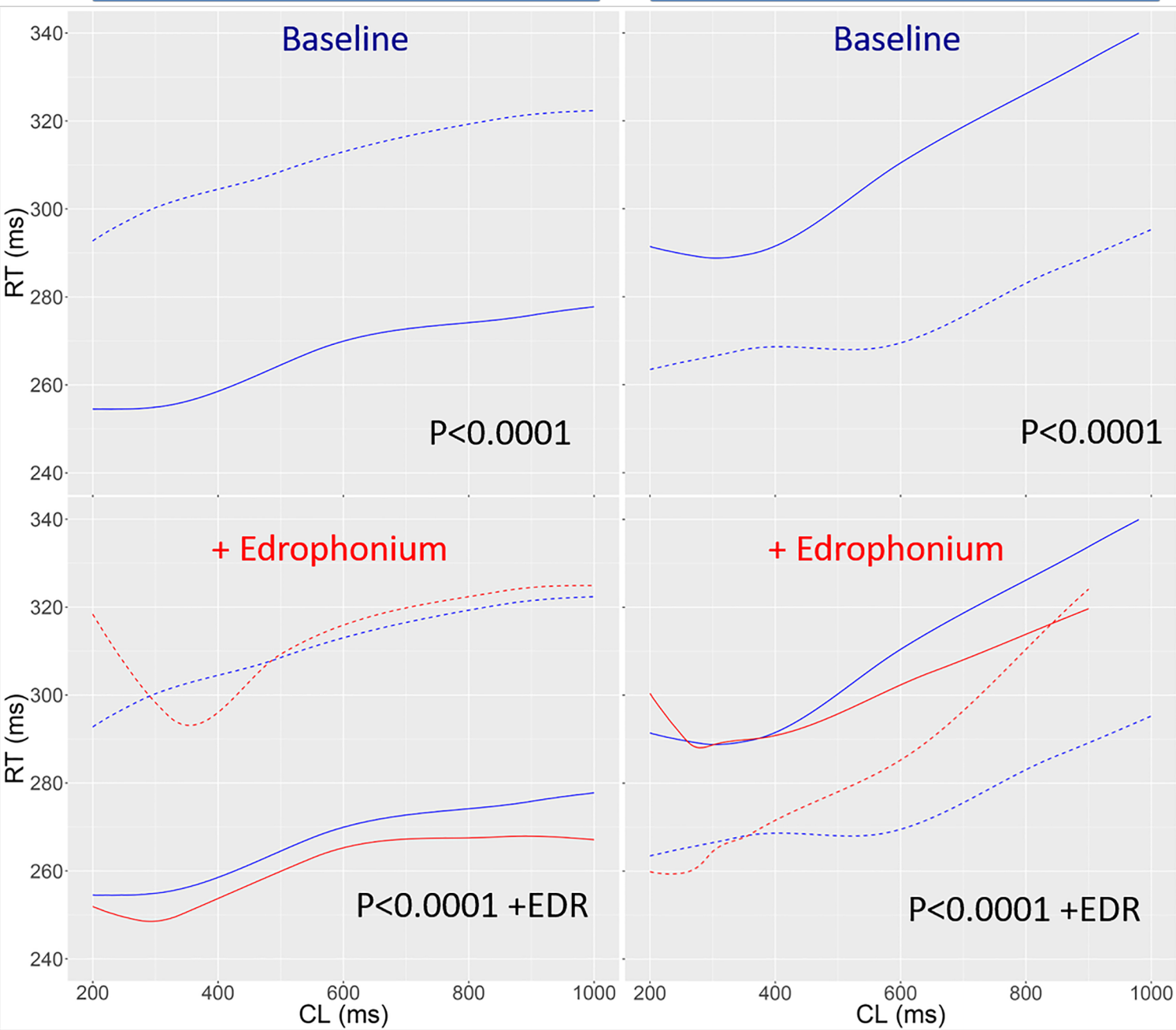
Base
Edr
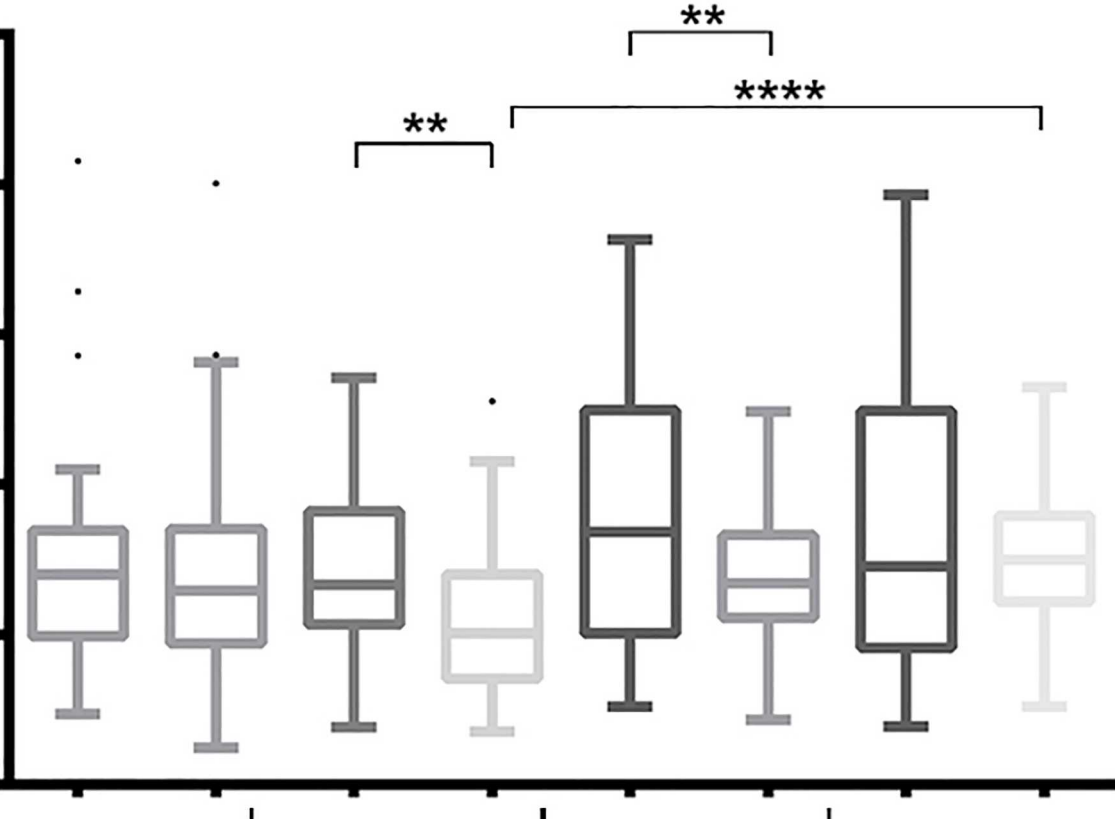
SUPPLEMENTAL MATERIAL
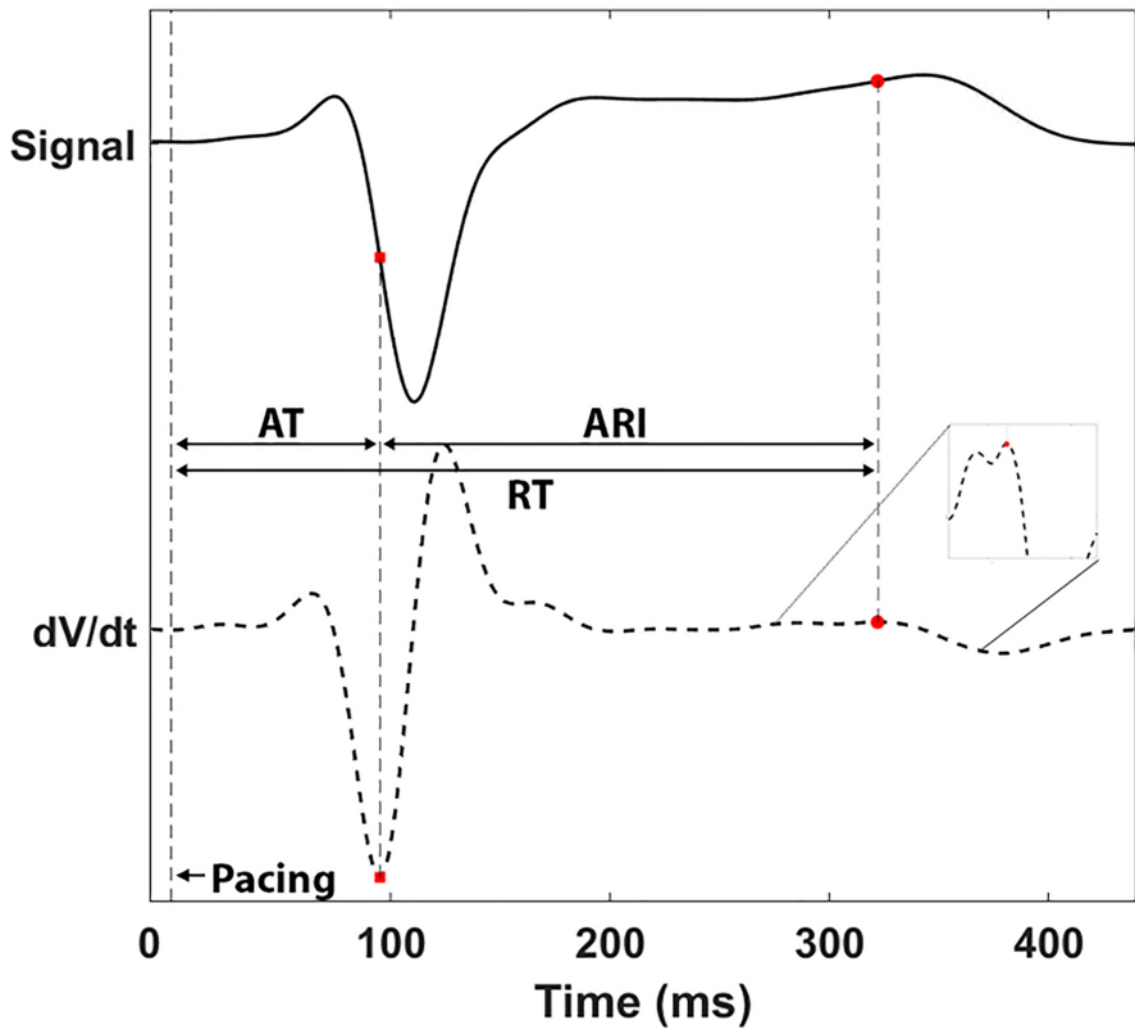
Supplemental Figure S1. Example of semi-automated AT, ARI and RT measurements from intracardiac Non-contact unipolar signals. The blue interrupted line is the dV/dt of the solid black line (which is the signal exported from Ensite NC mapping system). The red coloured squares mark activation times (dV/dt min) and the blue dV/dt max of the T wave upstroke to measure ARI: the Wyatt method was used to look at all T waves employing upstroke of the T wave.
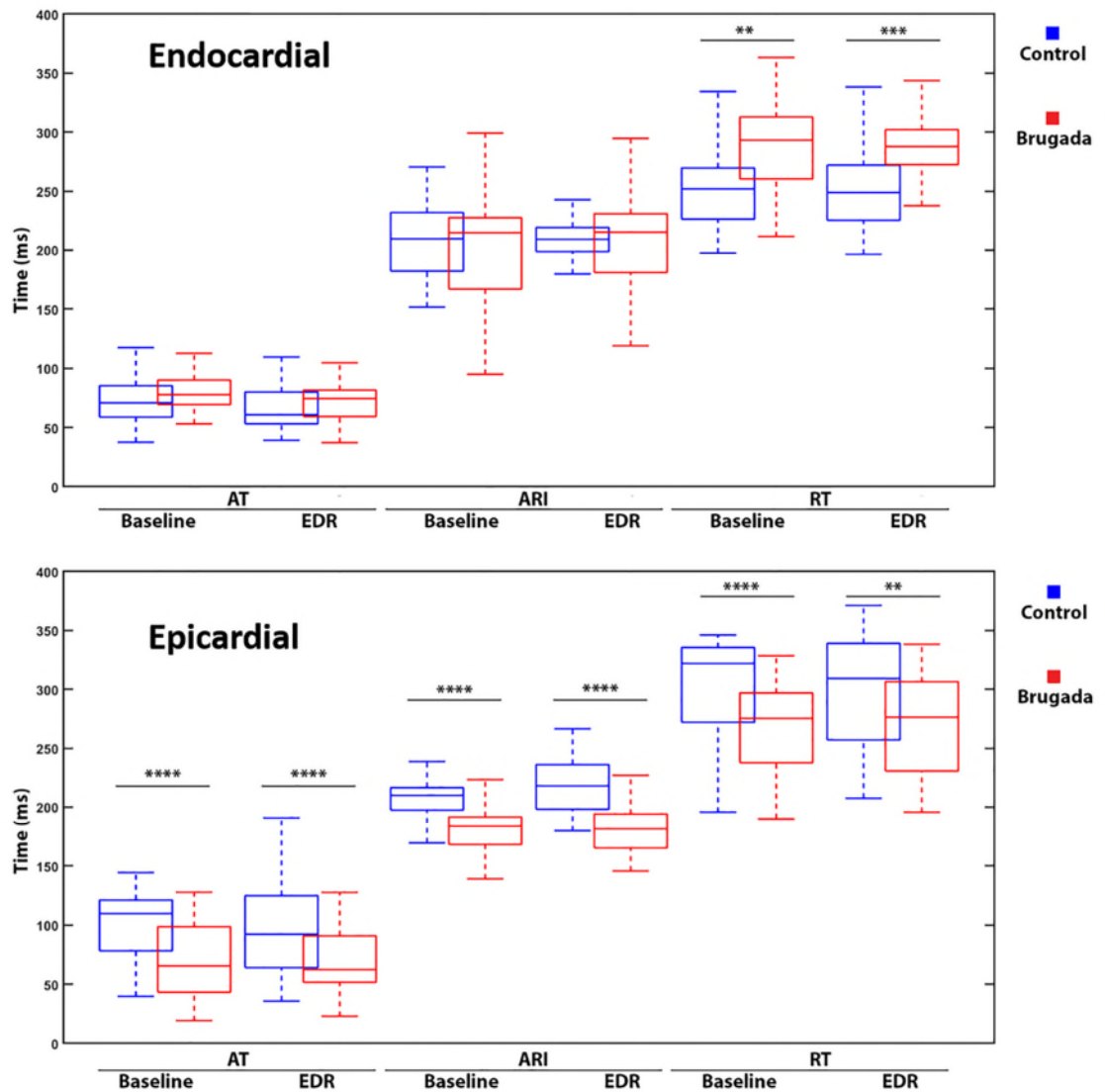
Supplemental Figure S2. A. Baseline Epicardial AT, ARI and RT in Controls and BrS during steady state pacing at 400ms. *P<0.05 between control and BrS. **B.** Baseline Endocardial AT, ARI and RT in Controls and BrS during steady state pacing at 400ms. ***P<0.001, ** P< 0.01 between control and BrS.